Analysis of inspiratory and expiratory muscles using ultrasound in rats: A reproducible and non-invasive tool to study respiratory function

Abdallah Fayssoil, Pauline Michel-Flutot, Frédéric Lofaso, Robert Yves Carlier, Mostafa El Hajjam, Stéphane Vinit, Arnaud Mansart

Analysis of inspiratory and expiratory muscles using ultrasound in rats: A reproducible and non-invasive tool to study respiratory function

Abdallah FAYSSOIL [1,2], Pauline MICHEL-FLUTOT [1], Frédéric LOFASO [1,2], Robert CARLIER [1,3], Mostafa EL HAJJAM [4], Stéphane VINIT [1], Arnaud MANSART [5]

1. University of Paris-Saclay, UVSQ, INSERM U1179, END-ICAP, Montigny-le-Bretonneux, France.

2. Raymond Poincaré Hospital, APHP, Garches, France

3. APHP, GH Université Paris Saclay, DMU Smart Imaging, Raymond Poincaré Teaching hospital, Garches, France

4. Radiology department, Ambroise Paré Hospital, APHP, Boulogne-Billancourt, France

5. University of Paris-Saclay, UVSQ, INSERM U1173, 2I, Montigny-le-Bretonneux, France

Corresponding author:

Arnaud MANSART, PhD
University of Paris-Saclay, UVSQ, INSERM U1173, 2I, Montigny-le-Bretonneux, France.
E-mail: arnaud.mansart@uvsq.fr
Phone: +33 1 70 42 94 14

Abstract

Ultrasound imaging is a non-invasive technique to assess organ function. Its potential application in rodents to evaluate respiratory function remains poorly investigated. We aimed to assess and validate ultrasound technique in rats to analyze inspiratory and expiratory muscles. We measured respiratory parameters to provide normal eupneic values. Histological studies and plethysmography were used to validate the technique and assess the physiological implications. A linear relationship was observed between ultrasound and histological data for diaphragm and rectus abdominis (RA) measurement. The tidal volume was significantly correlated with the right + left RA area ($r=0.76$, $p<0.001$), and the rapid shallow breathing index was significantly and inversely correlated with the right + left RA area ($r=-0.53$, $p<0.05$). In the supine position, the right and left diaphragm expiratory thickness were not associated with tidal volume obtained in the physiological position. Ultrasound imaging is highly accurate and reproducible to assess and follow up diaphragm and RA structure and function in rats.

Keywords

Ultrasound; Rat; Diaphragm; Rectus abdominis

1. INTRODUCTION

Ultrasound imaging is a non-invasive technique to assess organ function, particularly the heart (Coatney, 2001). In animal studies, this technique is used to assess left ventricular systolic function (Fayssoil and Tournoux, 2013) but remains uncommon for other organs. Usually, lung and respiratory muscle functions in animals are assessed indirectly by plethysmography (Lim et al., 2014). This technique is often used to evaluate respiratory dysfunction in neuromuscular disorders or after cervical spinal cord injury (Goyenvalle et al., 2015; Wen et al., 2019). Respiratory muscle function analyses in animals also rely on *ex vivo* measurements of isometric force, or *in vivo* electromyography recordings of the diaphragm in anesthetized animals or using telemetry implants in awake animals (Navarrete-Opazo et al., 2015; Vinit et al., 2006). However, these techniques are invasive, cannot provide longitudinal studies, and for the terminal recordings, require sacrifice of the animals. The development of non-invasive tools for evaluating respiratory function in animal models is necessary and will be useful to assess potential therapeutic applications.

Ultrasound is already used to assess respiratory muscles in humans (Boussuges et al., 2009; Scarlata et al., 2018; Ueki et al., 1995). Among these, the diaphragm is considered the main inspiratory muscle. In preclinical models, several studies have proven the efficacy of ultrasonography to evaluate diaphragmatic function in a canine model of muscular myopathy (Sarwal et al., 2014), diaphragmatic wild-type mice (Zuo et al., 2014), fetal breathing movements in rats (Kobayashi et al., 2001), and a neuromuscular-disordered mouse model of Duchenne dystrophy (Whitehead et al., 2016). However, the expiratory muscles also participate actively in the respiratory behavior, including the rectus abdominis (RA), external obliques (EO), internal obliques (IO), and transversus abdominis (TA) especially for rodents and dogs. Functional activity and efficacy of these respiratory-related muscles can be affected in the case of heavy pathologies such as spinal cord injury (Laghi and Tobin, 2003).

To date, no data have been reported regarding the evaluation of several respiratory-related muscles or even expiratory muscles by ultrasound in a rat model. The present study depicts and evaluates in anesthetized rats using ultrasound technique the physiological values of the

diaphragm muscle (thickness, thickening, and inspiratory motion) and RA muscle thickness. Taken together, these data provide a reference for diaphragm and RA ultrasound measurements in eupneic conditions in control rats.

2. METHODS

2.1. Animals

All experiments were performed in accordance with French laws concerning animal experimentation (20171115162973O8V3) and were approved by our Institutional Animal Care and Use Committee (C2EA-47). Adult male Sprague Dawley rats (Janvier, Le Genest-Saint-Isle, France) were acclimated on arrival at a constant temperature (22 °C) and exposed to a 12–12 hour light–dark cycle for a minimum of 7 days before any experimentation was performed. They were maintained in a pathogen-free environment with access to food and water ad libitum during the experimental procedure.

2.2. Experimental protocol

Initially, 4 control rats (291–300 g body weight) without cardiopulmonary disease were included in this study to validate the ultrasound technique. Different parameters using ultrasound were measured under anesthesia (1.5–2% isoflurane, balanced with 100% O_2): right and left diaphragm thickness at end expiration and end inspiration in animals on quiet spontaneous ventilation, and right and left RA thickness and area during quiet spontaneous ventilation.

Then, 15 rats (330–599 g body weight) were included to confirm our previous observations and increase statistical power. These additional animals were used to provide basal values for diaphragm thickness, thickening, and inspiratory motion, as well as values for RA thickness. 13 of these 19 animals were also used for RA area measurements.

Plethysmography, ultrasound recordings, and histological studies were used with this approach for each animal.

2.3. Whole-body plethysmography

Whole-body constant flow (0.5 L/min) plethysmography (EMKA, France) was used to assess global ventilatory function (e.g., tidal volume, minute ventilation, and breathing frequency) in our animals, as previously described (Wen et al., 2019) (Figure 1D). The system was first calibrated and the rats weighed. After a 30-minute acclimation period in the chambers, the recording began under normoxic conditions (room air). Tidal volume and minute ventilation were reported by body weight (per 100g) for each animal. Calculation of the rapid shallow breathing index (RSBI: respiratory rate [RR]/tidal volume) was performed. This index reflects the work of breathing and has already been assessed in patients with neuromuscular disorders (Misuri et al., 2000).

2.4. Diaphragm and rectus abdominis ultrasound

Respiratory muscle function was evaluated using a high-resolution ultrasound system (LOGIQ E9; GE, France) and a linear L8-18i probe (GE, France) at high frequency (18 MHz; Figure 1B, 1C). All animals were anesthetized by isoflurane (Forene®; Abbott, France) at a concentration of 5% for induction in a chamber (Figure 1A) at 500 cc/minute in 100% oxygen. The isoflurane concentration was subsequently reduced to 1.5–2% (balanced with 100% O_2) for maintenance during handling and ultrasound.

Each animal's anterior thorax and upper abdomen was shaven with depilatory cream before exploration. Then, the animal was placed in the supine position on the imaging platform, and body temperature was continuously monitored using a rectal probe and maintained at 37 ± 0.5 °C. Ultrasound gel was applied to the chest of the rat before diaphragm and RA measurements.

M mode ultrasound was used to assess diaphragm motion from the subcostal view after visualization of the diaphragm (Figure 2). Diaphragmatic inspiratory motion, inspiratory time, and expiratory time, from the M mode, were recorded (Figure 2B and 2C).

2D mode was used to assess diaphragm thickness and thickening from the apposition zone during live breathing. For this setting, the probe was placed perpendicularly to the chest wall

at the midaxillary line to visualize the costophrenic sinus. In this apposition zone, a clear visualization of the diaphragm can be recorded, bounded by 2 clear bright lines: the pleural line and the peritoneal line (Figure 3). The thicknesses of the diaphragm at the end of the expiration and inspiration cycles were also recorded. Thickening fraction (TF) of the diaphragm was calculated using this ratio: ([thickness at end inspiration]-[thickness at end expiration])/[thickness at end expiration] (Matamis et al., 2013).

For the RA analysis, the probe was held vertically on the upper abdomen, just above the umbilicus, then moved over to have the linea alba in the middle. The right and left RA muscles were easily visualized (on each side of the linea alba, surrounded by the muscle sheaths) and the thickness and area were measured (Figure 3B).

2.5. Histological analysis

The animals were anesthetized with 5% isoflurane and received an intracardiac injection of Exagon (1 mL/kg).The animals were perfused with heparinized saline (0.9% NaCl) and the diaphragm and RA were dissected out and frozen in isopentane (-45 °C). Transverse frozen sections (7 µm thickness) using a cryostat (Leica) were collected and hematoxylin–eosin stained. Slides were scanned (Leica Scanner, France), and each section was analyzed with ImageJ software (NIH). The thickness and area of the diaphragm and RA were measured. For the diaphragm thickness, 5 different locations were measured and averaged for the same section per animal. For the RA, the thickness was measured at the largest location for each animal.

2.6. Statistical analysis

Data were expressed as mean ± SD. Statistical significance was defined as $p < 0.05$. All significant p-values were obtained with a power analysis better than 80%. Ultrasound imaging was performed by 2 operators with skill in animal ultrasound imaging (Fayssoil and Tournoux, 2013). To test the intra-operator agreement (reproducibility) of ultrasound measurements, one observer performed measurements 5 times within 1 hour apart. To test

the inter-operator agreement (variability), 2 observers performed the measurements separately. To test the agreement between ultrasound and histological measurements, the method described by Bland and Altman was used (Misuri et al., 1997), including 95% limits of agreement (LOA). The LOA define the intervals within which we can be 95% confident that the respective measurements will lie considering their relative variability; hence, the narrowest LOA characterizes the method with the best agreement. In addition, the mean difference between the 2 techniques (bias) was calculated, along with SD. To test intra- and inter-observer agreement, a Bland–Altman plot was used as well. Statistical analysis also involved Spearman's correlation and logistic regression. A student t-test was performed to compare histological and ultrasound values obtained on the same samples. XLSTAT PREMIUM 2016.1.1 (Addinsoft statistical and data analysis solution. Paris, France. https://www.xlstat.com) was used for all statistical analyses.

3. RESULTS

3.1. Whole-body plethysmography in unanesthetized rats

14 of the 19 animals were included in this study. Inspiratory time (199 ± 39 ms), expiratory time (396 ± 133 ms), minute ventilation (44.01 ± 10.52 mL/min/100g), tidal volume (0.39 ± 0.03 mL/100g) and respiratory rate (113 ± 23 breaths/min) were recorded. The Rapid Shallow Breathing index (RSBI) was also calculated as described in the method section. All results are shown in Table 1.

3.2. Intra-operator reproducibility and inter-operator variability for ultrasound measurements

Inter-operator variability and intra-operator reproducibility are shown in Table 2. These agreements were tested with the 4 first animals. We found a high mean correlation coefficient for all the parameters studied (combinations of area and thickness for the RA or thickness and motion for the diaphragm muscle). Coefficients of variation were between 1.06 (right diaphragm inspiratory motion) and 5.87% (right diaphragm inspiration thickness) for the

operator n°1 *versus* 1.44 (right rectus abdominis thickness) and 7.66% (right diaphragm inspiration thickness) for the operator n°2.

3.3. Diaphragm ultrasound

A total of 19 animals were included in this study. Using the high-resolution ultrasound system, the diaphragm end expiratory thickness was 0.74 ± 0.06 mm for the right hemi-diaphragm, similar to the histological finding (0.84 ± 0.03 mm). A linear relationship (r = 0.75, p = 0.02) was observed between ultrasound and histological data. The left hemi-diaphragm thickness at end expiration was 0.78 ± 0. 10 mm measured by ultrasound, while with histological analysis, the diaphragm thickness was 0.88 ± 0.05 mm, again with a linear relationship (r = 0.45, p = 0.12) between these 2 different methods of evaluation.

The diaphragm TF was similar for the 2 hemi-diaphragms: 23.54 ± 5.95 % for the right hemi-diaphragm and 23.37 ± 6.17 % for the left hemi-diaphragm. The diaphragm inspiratory motion was also similar for the 2 hemi-diaphragms: 4.04 ± 0.59 mm for the right hemi-diaphragm and 4.28 ± 0.95 mm for the left hemi-diaphragm.

3.4. Rectus abdominis ultrasound

A total of 19 animals were included in the thickness measurement. Using ultrasound, the mean thickness of the RA, during anesthetized quiet poikilocapnic breathing, was 1.55 ± 0.11 mm for the right RA and 1.59 ± 0.12 mm for the left RA. Histological values for mean RA thickness were 2.44 ± 0.30 mm for the right RA and 2.27 ± 0.22 mm for the left RA. A linear relationship between ultrasound data and histological data was observed for both sides (r = 0.7, p = 0.001 for the right RA; r = 0.48, p = 0.001 for the left RA).

Similar findings regarding RA area were observed between the 2 methods of analyses (ultrasound vs histological values; mean right ultrasound RA area 23.00 ± 1.02 mm^2 vs 21.90 ± 1.95 mm^2 with histology [p = 0.35]; mean left ultrasound RA area 22.79 ± 1.00 mm^2 vs 21.78 ± 0.60 mm^2 with histology [p = 0.13]). This analysis of RA area was realized on 13 animals.

3.5. Histology of diaphragm and rectus abdominis

Examination of diaphragm and RA muscles stained with hematoxylin–eosin was used to determine size-related parameters in the rats (Figure 4). The diaphragm thickness was 0.84 ± 0.03 mm for the right side and 0.88 ± 0.5 mm for the left side. For the RA, the muscle thickness was 2.44 ± 0.30 mm for the right side and 2.27 ± 0.22 mm for the left side. The muscle area was 21.90 ± 1.95 mm^2 for the right side and 21.78 ± 0.65 mm^2 for the left side.

3.6. Ultrasound and histological agreement and correlation

Using the ultrasound method, the left RA area was 22.80 ± 1.00 mm^2, while the histology-derived left RA area was 21.78 ± 0.65 mm^2. For the right RA, the area was 23.00 ± 1.02 mm^2, and the histology-derived left RA area was 21.90 ± 1.95 mm^2. Comparison between ultrasound and histological values did not display significant difference. The mean biases (95% confidence intervals) were 1.02 (-0.79 to 2.82) and 1.1 (-4.42 to 6.62), respectively (Table 3).

3.7. Relationship between rectus abdominis area, tidal volume, and rapid shallow breathing index

The tidal volume was significantly correlated with the right + left RA area ($r = 0.76$, $p < 0.001$) (Figure 5). The RSBI was also significantly and negatively correlated with the right + left RA area ($r = -0.53$, $p < 0.05$) (Figure 6).

3.8. Relationship between diaphragm and rapid shallow breathing index

In the supine position, the right and left diaphragm expiratory thicknesses were not associated with tidal volume (respectively $p = 0.89$ and $p = 0.5$). Further, the diaphragm TF was not associated with tidal volume ($p = 0.54$ for the right TF and $p = 0.37$ for the left TF). The RSBI index was inversely but not significantly associated with right + left diaphragm thickness ($r = -0.17$, $p = 0.39$) (Figure 7).

4. DISCUSSION

This is the first study in rats to report data about diaphragm and RA thickness or area obtained with a non-invasive ultrasound technique, validated by post-mortem histological analyses. In addition, in our rat model, the data support the high reproducibility of this technique for the assessment of diaphragm and RA muscle evaluation.

The echographic findings were validated by the histological findings and previous reports by Farkas about diaphragm thickness (Farkas et al., 1994) and Jeong about rat RA muscle (Jeong et al., 2017). In humans, Wait et al. (Wait et al., 1989) reported in 1989 ultrasound data about diaphragmatic thickness, validated by necropsy studies, with high correlation ($r = 0.93$, $p < 0.001$). This present study found a similar correlation between ultrasound and histological data in rats, using an ultrasound probe with high resolution frequency. The bias found in our study (1 for the left RA and 1.1 for the right RA) may be explained by the histological processing of the tissue before hematoxylin–eosin staining, as the unfixed muscle tissue slices must be dehydrated before staining. On the other hand, the ultrasound probe hold over the muscle could artificially reduce the size of the tissue. Moreover, the animals were alive, so even if we analyzed the size during the muscle relaxation, the muscle would not be fully relaxed. Therefore, the values obtained with the ultrasound technique are close to the histological values and real physiological measures. Our observations underscore the usefulness of ultrasound imaging for the assessment of respiratory muscle in live animals, with the possibility of repeated measures over time.

Ultrasound has previously been used to assess diaphragm function in mice (Zuo et al., 2014), particularly for mdx mice, with significant a correlation between diaphragm inspiratory motion and *ex vivo* specific force values (Whitehead et al., 2016). In this study, no *ex vivo* data were reported for the diaphragm or RA. However, significant correlations have been demonstrated between ultrasound measurements in anesthetized animals and plethysmography in conscious animals. Inspiratory time, expiratory time, tidal volume, minute ventilation and respiratory rate values reported in this present study for eupneic quiet

breathing in conscious animals were similar to values reported in the literature (Fuller et al., 2008; Lee et al., 2014; Lovett-Barr et al., 2012).

Tidal volume measured in non-anesthetized rats was significantly associated with RA area and thickness. This finding suggests that these muscles are involved during the eupneic respiratory cycle in conscious rats. One explanation may be the anti-gravitational role of these muscles in rats, located in the ventral position, and responsible for maintaining the viscera inside the peritoneal cavity. In humans, during expiratory efforts, expiratory muscles are solicited with a significant increase in thickness, including the RA, TA, and IO (Misuri et al., 1997). The thickness of the TA was particularly related to the gastric pressure developed during expiratory effort. Indeed, the TA muscle is disposed circumferentially in the abdomen, facilitating the increase of gastric pressure during expiratory effort (De Troyer et al., 1989). At residual volume, an increase in thickness has been reported for the RA, IO, and TA in humans (Misuri et al., 1997). In animals, De Troyer et al. (De Troyer et al., 1989) reported data about respiratory muscles, using electromyograms in conscious dogs during quiet breathing, and confirmed that the TA was the main expiratory muscle involved. In our study, the RA seemed more solicited to maintain tidal volume in the supine ventral position in rats, evidenced by the positive association between the RA area and the tidal volume.

Rats with a high RA area showed a reduced respiratory load, evidenced by the inverse significant relationship between RSBI and RA area. This finding corroborates the fact that these muscles are more solicited in animals during the respiratory cycle. However, we cannot rule out that these muscles may be more solicited during anesthesia, since isoflurane reduces the activity of expiratory muscles.

Inversely, we found a negative relationship between diaphragm inspiratory motion and tidal volume. One explanation may be that these measurements were made in different physiological conditions. Diaphragm ultrasound investigations were performed on isoflurane-anesthetized rats in the supine dorsal position, whereas ventilatory parameters (tidal volume and respiratory frequency) were obtained in fully awake, quiet breathing rats in room air, positioned on their limbs. However, the RSBI seemed to be reduced in rats with an increase

of diaphragm thickness, suggesting a relationship between muscle thickness and respiratory loading.

The reference test for the assessment of diaphragm function relies on the measurement of transdiaphragmatic pressure in humans (Polkey, 2019). This technique was not performed in this study. Further, we focused our study on the diaphragm and RA, due to the feasibility to obtain imaging. We did not include the other abdominal muscles: EO, IO, and TA. The TA seems to be the major contributor in generating abdominal expiratory pressure during expiratory effort, but this evaluation remains complicated in control rats using ultrasound during anesthesia. The EO is preferentially involved during trunk rotation, without link with inspiratory or expiratory muscles.

5. Conclusion

Analysis of respiratory function is critical and needs to be explored with relevant parameters close to *in vivo* conditions. In animals, this analysis is limited to *ex vivo* measurements of isometric force, *in vivo* recording by invasive electromyography and telemetry implants, or indirect data from plethysmography. These techniques are often invasive, cannot provide longitudinal studies, and require sacrifice of the animals. The development of non-invasive tools to evaluate the respiratory function in rodent models is necessary and will be useful to assess potential therapeutic applications in humans. Our study provides this tool, proves the feasibility and relevance of ultrasound imaging to study respiratory parameters in rats, and provides a reference for future publications. These results expands on interesting perspectives, especially in animal models of respiratory impairments (such as cervical spinal cord injury or amyotrophic lateral sclerosis) with therapeutics.

Acknowledgments

Funding: This work was supported by funding from the Chancellerie des Universités de Paris (Legs Poix) (SV), the Fondation de France (SV), the Fondation Médisite (SV), INSERM (SV,

AM) and Université de Versailles Saint-Quentin-en-Yvelines (SV, AM). The supporters had no role in study design, data collection and analysis, decision to publish, or preparation of the manuscript.

Declarations of interest: none

REFERENCES

Boussuges, A., Gole, Y., Blanc, P., 2009. Diaphragmatic motion studied by m-mode ultrasonography: methods, reproducibility, and normal values. Chest 135, 391-400.

Coatney, R.W., 2001. Ultrasound imaging: principles and applications in rodent research. ILAR J 42, 233-247.

De Troyer, A., Gilmartin, J.J., Ninane, V., 1989. Abdominal muscle use during breathing in unanesthetized dogs. Journal of applied physiology (Bethesda, Md. : 1985) 66, 20-27.

Farkas, G.A., Gosselin, L.E., Zhan, W.Z., Schlenker, E.H., Sieck, G.C., 1994. Histochemical and mechanical properties of diaphragm muscle in morbidly obese Zucker rats. Journal of applied physiology (Bethesda, Md. : 1985) 77, 2250-2259.

Fayssoil, A., Tournoux, F., 2013. Analyzing left ventricular function in mice with Doppler echocardiography. Heart Fail Rev 18, 511-516.

Fuller, D.D., Doperalski, N.J., Dougherty, B.J., Sandhu, M.S., Bolser, D.C., Reier, P.J., 2008. Modest spontaneous recovery of ventilation following chronic high cervical hemisection in rats. Experimental neurology 211, 97-106.

Goyenvalle, A., Griffith, G., Babbs, A., El Andaloussi, S., Ezzat, K., Avril, A., Dugovic, B., Chaussenot, R., Ferry, A., Voit, T., Amthor, H., Bühr, C., Schürch, S., Wood, M.J.A., Davies, K.E., Vaillend, C., Leumann, C., Garcia, L., 2015. Functional correction in mouse models of muscular dystrophy using exon-skipping tricyclo-DNA oligomers. Nat Med 21, 270-275.

Jeong, W.S., Lee, S.S., Park, E.J., Han, J.J., Choi, J.W., Koh, K.S., Oh, T.S., 2017. Comparison of Biomechanical and Histological Outcomes of Different Suture Techniques in Rat Rectus Abdominis Muscle Repair. Ann Plast Surg 78, 78-82.

Kobayashi, K., Lemke, R.P., Greer, J.J., 2001. Ultrasound measurements of fetal breathing movements in the rat. J Appl Physiol (1985) 91, 316-320.

Laghi, F., Tobin, M.J., 2003. Disorders of the respiratory muscles. Am J Respir Crit Care Med 168, 10-48.

Lee, K.Z., Huang, Y.J., Tsai, I.L., 2014. Respiratory motor outputs following unilateral midcervical spinal cord injury in the adult rat. J Appl Physiol (1985) 116, 395-405.

Lim, R., Zavou, M.J., Milton, P.-L., Chan, S.T., Tan, J.L., Dickinson, H., Murphy, S.V., Jenkin, G., Wallace, E.M., 2014. Measuring respiratory function in mice using unrestrained whole-body plethysmography. J Vis Exp, 51755.

Lovett-Barr, M.R., Satriotomo, I., Muir, G.D., Wilkerson, J.E., Hoffman, M.S., Vinit, S., Mitchell, G.S., 2012. Repetitive intermittent hypoxia induces respiratory and somatic motor recovery after chronic cervical spinal injury. The Journal of neuroscience : the official journal of the Society for Neuroscience 32, 3591-3600.

Matamis, D., Soilemezi, E., Tsagourias, M., Akoumianaki, E., Dimassi, S., Boroli, F., Richard, J.-C.M., Brochard, L., 2013. Sonographic evaluation of the diaphragm in critically ill patients. Technique and clinical applications. Intensive Care Med 39, 801-810.

Misuri, G., Colagrande, S., Gorini, M., Iandelli, I., Mancini, M., Duranti, R., Scano, G., 1997. In vivo ultrasound assessment of respiratory function of abdominal muscles in normal subjects. Eur Respir J 10, 2861-2867.

Misuri, G., Lanini, B., Gigliotti, F., Iandelli, I., Pizzi, A., Bertolini, M.G., Scano, G., 2000. Mechanism of CO(2) retention in patients with neuromuscular disease. Chest 117, 447-453.

Navarrete-Opazo, A., Vinit, S., Dougherty, B.J., Mitchell, G.S., 2015. Daily acute intermittent hypoxia elicits functional recovery of diaphragm and inspiratory intercostal muscle activity after acute cervical spinal injury. Experimental neurology 266, 1-10.

Polkey, M.I., 2019. Respiratory Muscle Assessment in Clinical Practice. Clin Chest Med 40, 307-315.

Sarwal, A., Cartwright, M.S., Walker, F.O., Mitchell, E., Buj-Bello, A., Beggs, A.H., Childers, M.K., 2014. Ultrasound assessment of the diaphragm: Preliminary study of a canine model of X-linked myotubular myopathy. Muscle & nerve 50, 607-609.

Scarlata, S., Mancini, D., Laudisio, A., Benigni, A., Antonelli Incalzi, R., 2018. Reproducibility and Clinical Correlates of Supine Diaphragmatic Motion Measured by M-Mode Ultrasonography in Healthy Volunteers. Respiration 96, 259-266.
Ueki, J., De Bruin, P.F., Pride, N.B., 1995. In vivo assessment of diaphragm contraction by ultrasound in normal subjects. Thorax 50, 1157-1161.
Vinit, S., Gauthier, P., Stamegna, J.C., Kastner, A., 2006. High cervical lateral spinal cord injury results in long-term ipsilateral hemidiaphragm paralysis. Journal of neurotrauma 23, 1137-1146.
Wait, J.L., Nahormek, P.A., Yost, W.T., Rochester, D.P., 1989. Diaphragmatic thickness-lung volume relationship in vivo. Journal of applied physiology (Bethesda, Md. : 1985) 67, 1560-1568.
Wen, M.-H., Wu, M.-J., Vinit, S., Lee, K.-Z., 2019. Modulation of Serotonin and Adenosine 2A Receptors on Intermittent Hypoxia-Induced Respiratory Recovery following Mid-Cervical Contusion in the Rat. Journal of neurotrauma 36, 2991-3004.
Whitehead, N.P., Bible, K.L., Kim, M.J., Odom, G.L., Adams, M.E., Froehner, S.C., 2016. Validation of ultrasonography for non-invasive assessment of diaphragm function in muscular dystrophy. The Journal of physiology 594, 7215-7227.
Zuo, L., Roberts, W.J., Evans, K.D., 2014. Diagnostic ultrasound imaging of mouse diaphragm function. J Vis Exp, 51290.

Tables and figures

Figures

Figure 1: Overview of the equipment. (A) Anesthetic equipment for induction with inhalation chamber; (B) ultrasound equipment (GE LOGIC E9); (C) linear probe with high frequency (18 MHz); (D) whole-body plethysmograph equipment

Figure 2: (A) Representative trace of plethysmography recording in eupnea (B) Representative trace of ultrasound recording showing the movement of the diaphragm during two successive breathing cycles. The measurement of the diaphragm movement amplitude is shown for one respiratory cycle, as the difference (arrow) from the baseline (dashed line) to the peak (continuous line). (C) Diaphragm ultrasound using M mode (left) and 2D mode (right). Expiratory time is measured from the diaphragm M mode trace

Figure 3: (A) Measurement of the diaphragm thickness from the right apposition zone using ultrasound. (B) Representative image showing the anatomical structures observed by the ultrasound probe with the right and the left rectus abdominis visualization from a sub xyphoidal view. Scale bars: 2 mm

Figure 4: Representative section of diaphragm (A) and rectus abdominis (B), after transverse sections and hematoxylin-eosin stained

Figure 5: Relationship between Tidal Volume and rectus abdominis area. Each dot matches with right or left side for each animal (sample size (n) = 8).

Figure 6: Relationship between Rapid Shallow Breathing (RSBI) and rectus abdominis area. Each dot matches with right or left side for each animal (sample size (n) = 8).

Figure 7: Relationship between diaphragm end expiratory thickness and rapid shallow breathing (RSBI). Each dot matches with right or left side for each animal (sample size (n) = 14).

Tables

Table 1. Whole body plethysmography in unanesthetized eupneic rats. Inspiratory time (T_I), expiratory time (T_E), minute ventilation (V_M), tidal volume (V_T), RSBI (Rapid Shallow Breathing index), minimum (min) and maximum (max). CV = coefficient of variation. Sample size (n) = 14.

Table 2. Correlation Coefficient (CC) for reproducibility intra-operator and variability inter-operator. Sample size (n) = 4.

Table 3. Agreement and correlation between ultrasound and histology measurements.

A


HARVARD
APPARATUS
FORANE
FLUOVAC
HARVARD
APPARATUS
fair

B

C


L8-18i

D

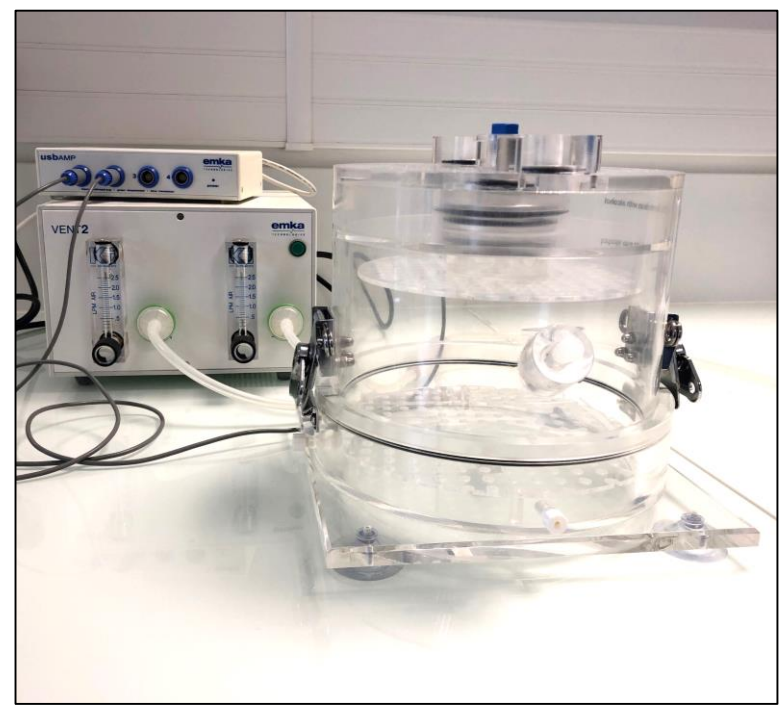
usbAMP
emka
emka

A

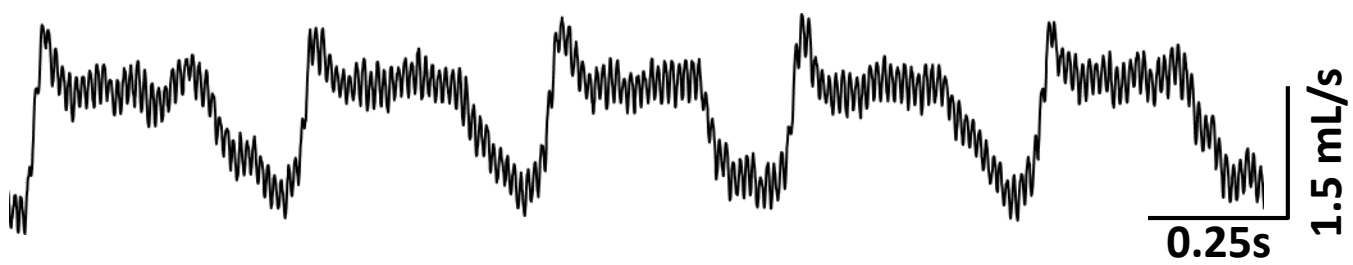
0.25s
1.5 mL/s

B

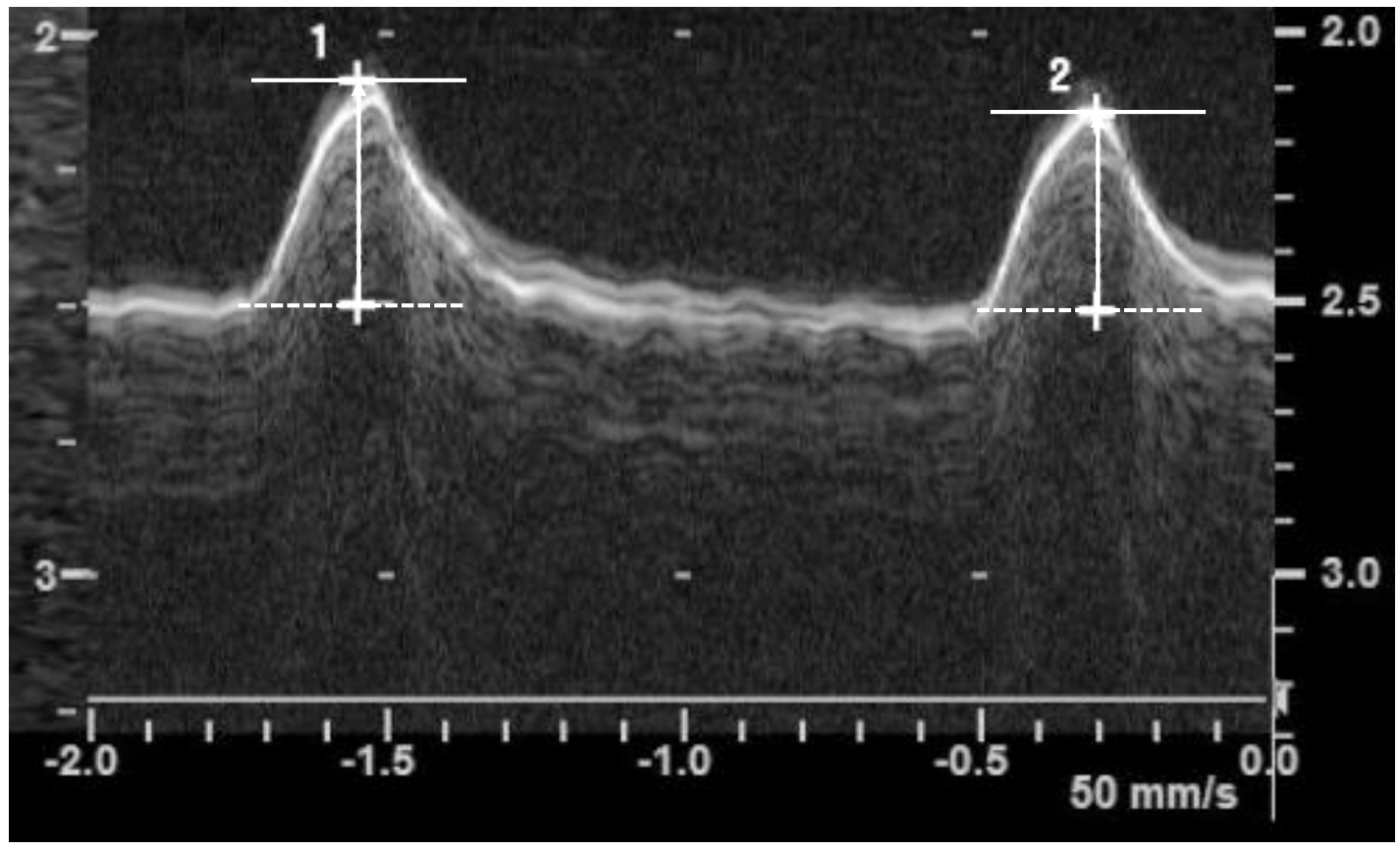
1
2
2.0
2.5
3.0
-2.0
-1.5
-1.0
-0.5
0.0
50 mm/s

C

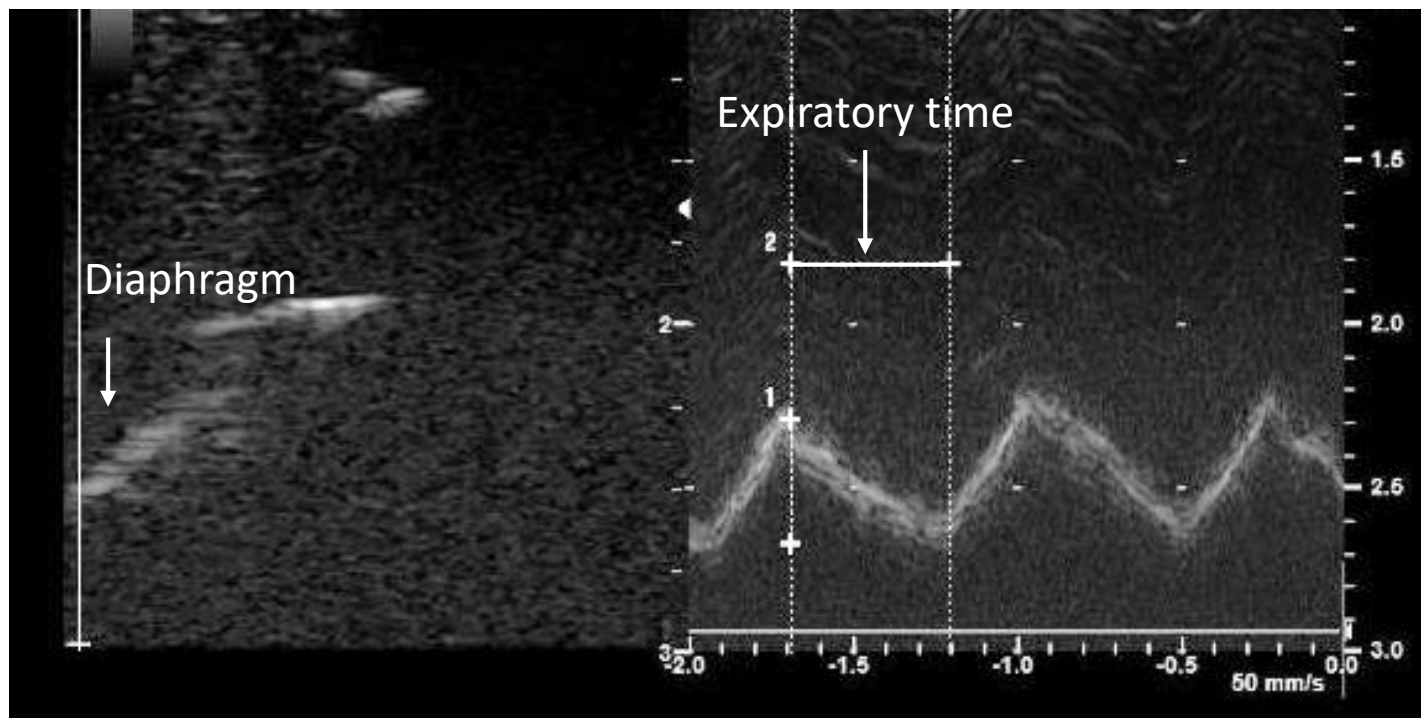
Diaphragm
Expiratory time
1
2
1.5
2.0
2.5
3.0
-2.0
-1.5
-1.0
-0.5
0.0
50 mm/s

A

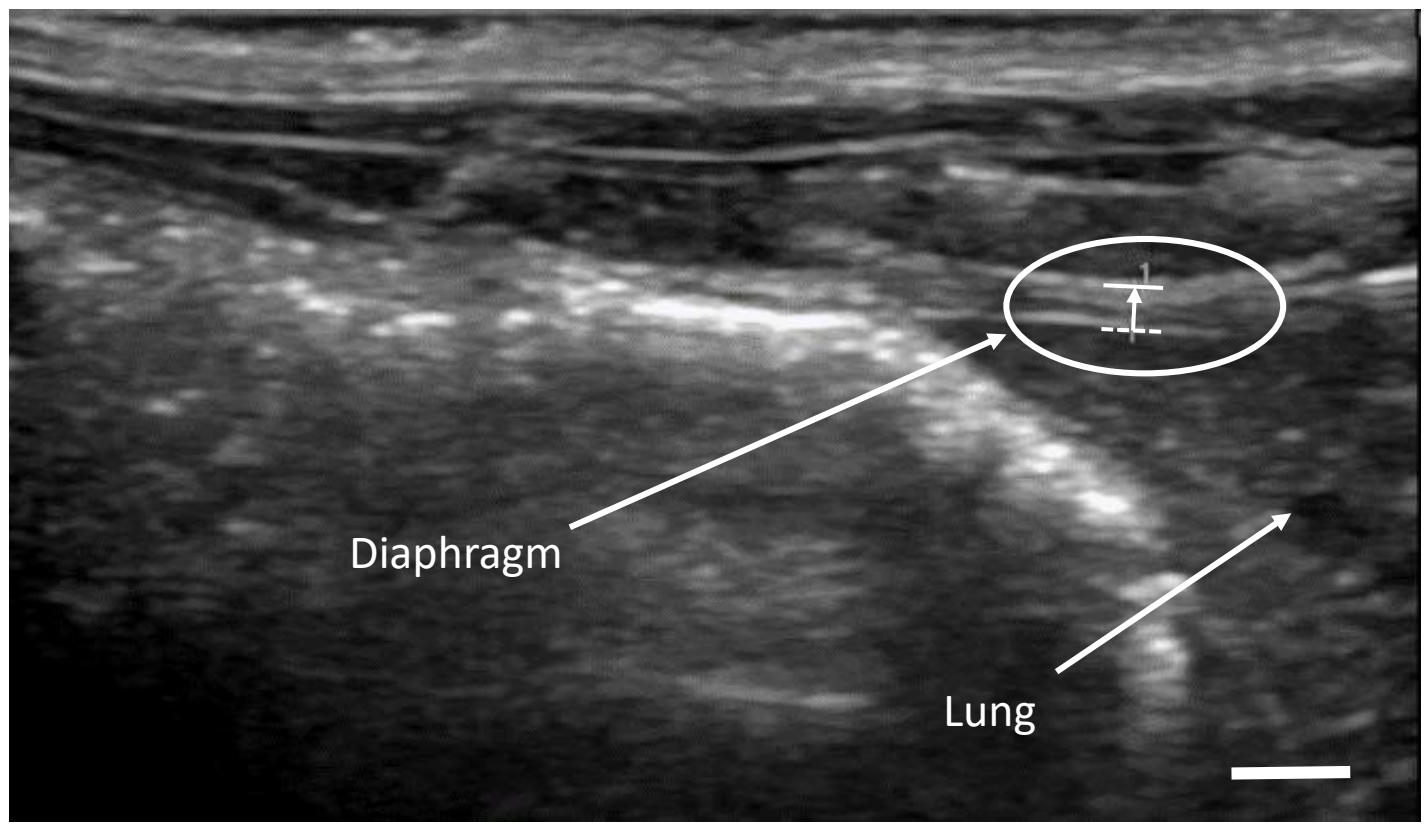

B

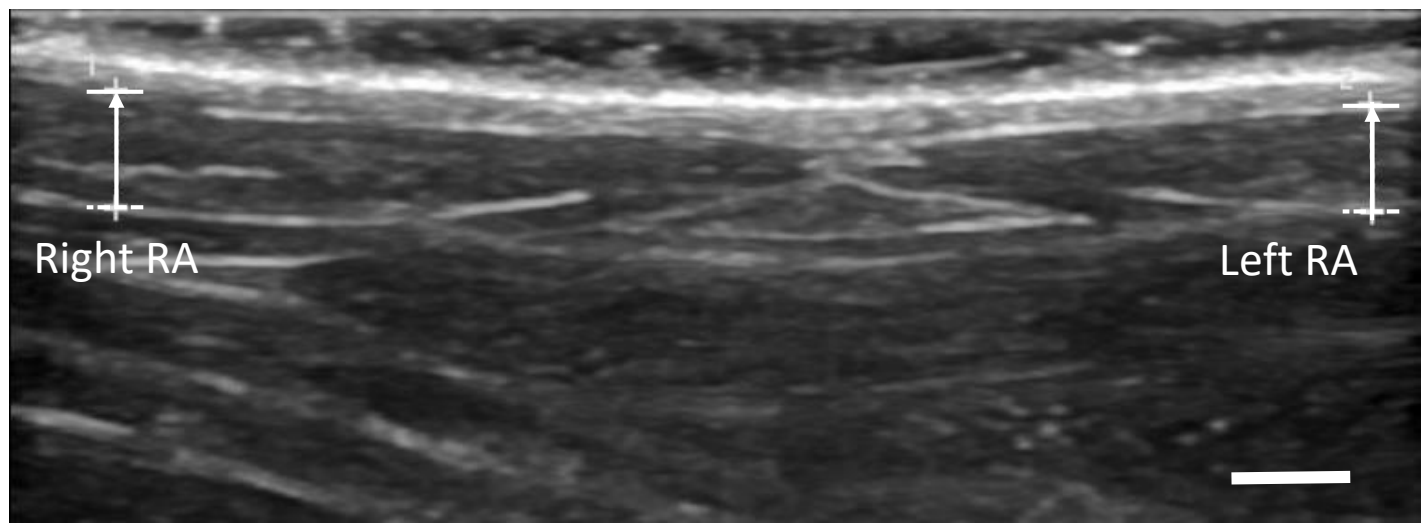

A

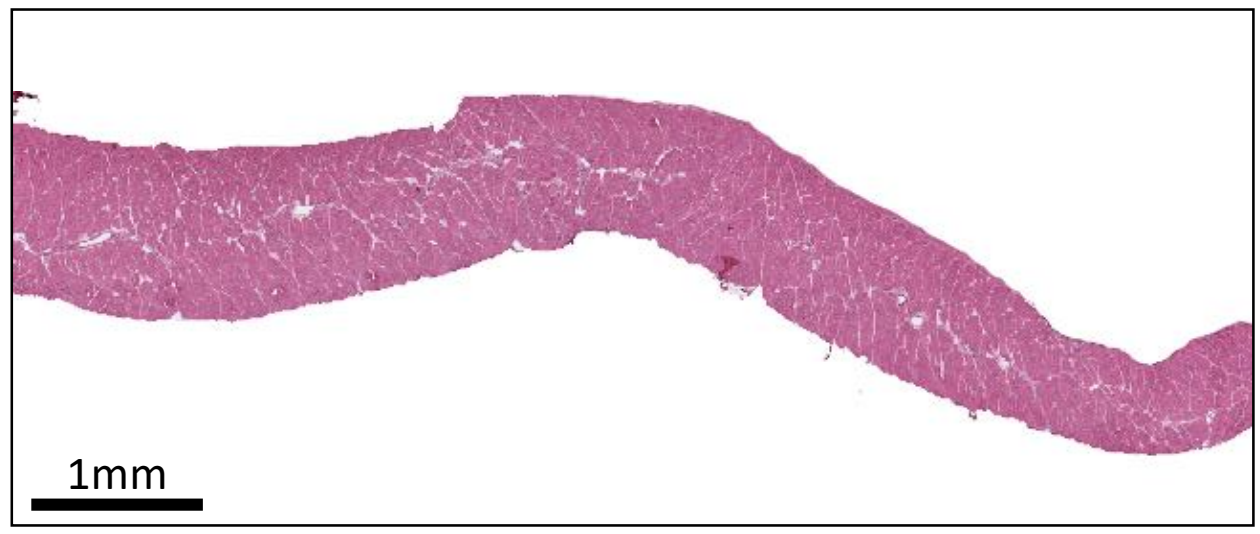

B

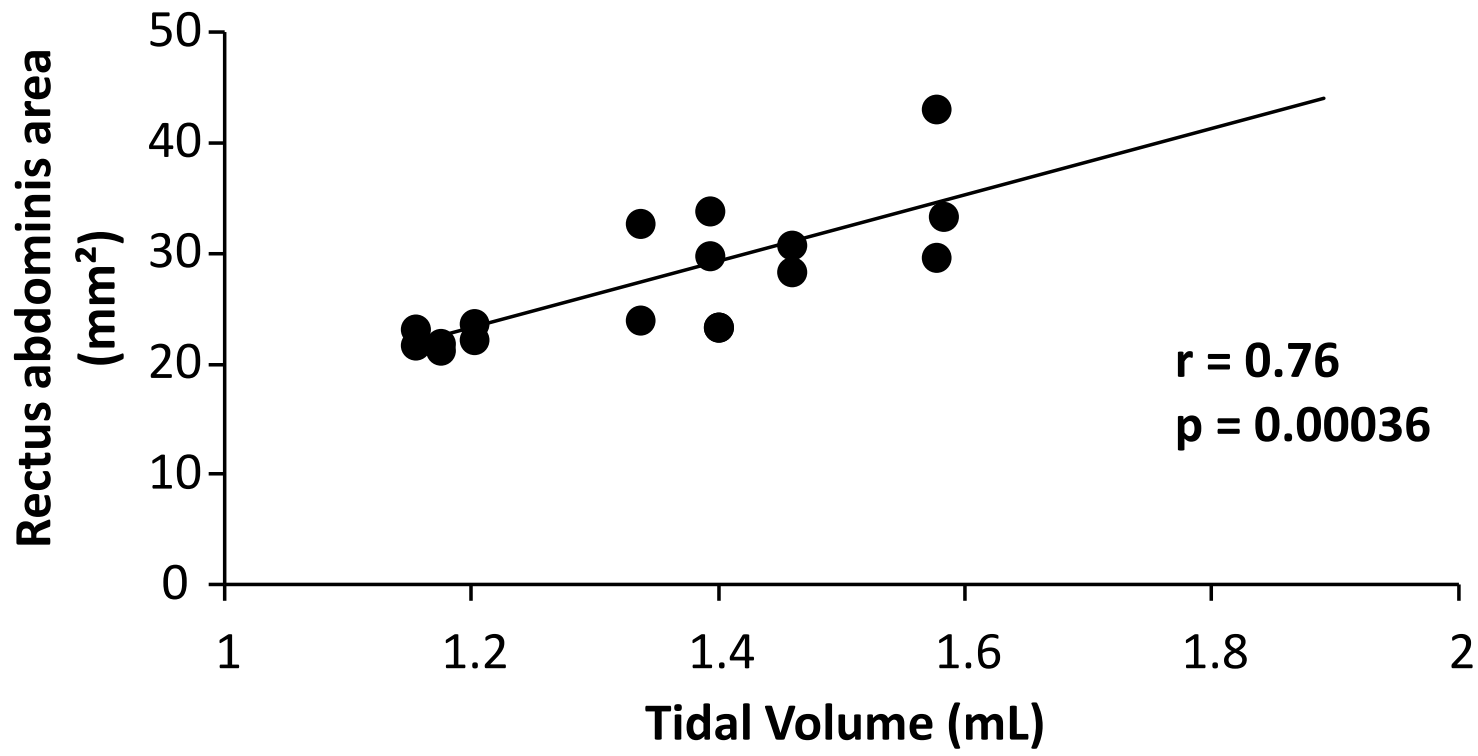
Rectus abdominis area (mm²)
50
40
30
20
10
0
1
1.2
1.4
1.6
1.8
2
Tidal Volume (mL)
r = 0.76
p = 0.00036

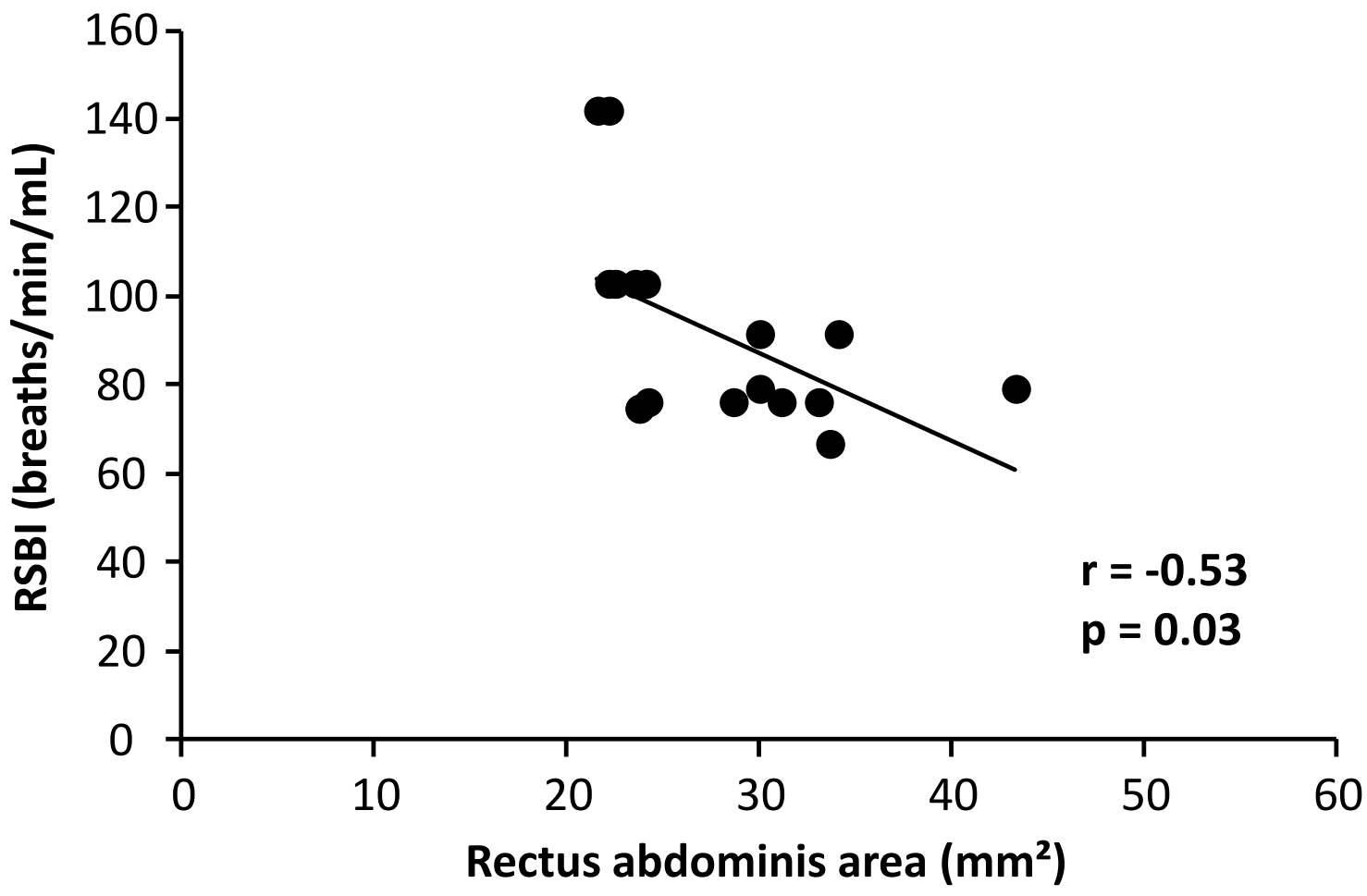
RSBI (breaths/min/mL)
160
140
120
100
80
60
40
20
0
0
10
20
30
40
50
60
Rectus abdominis area (mm²)
r = -0.53
p = 0.03

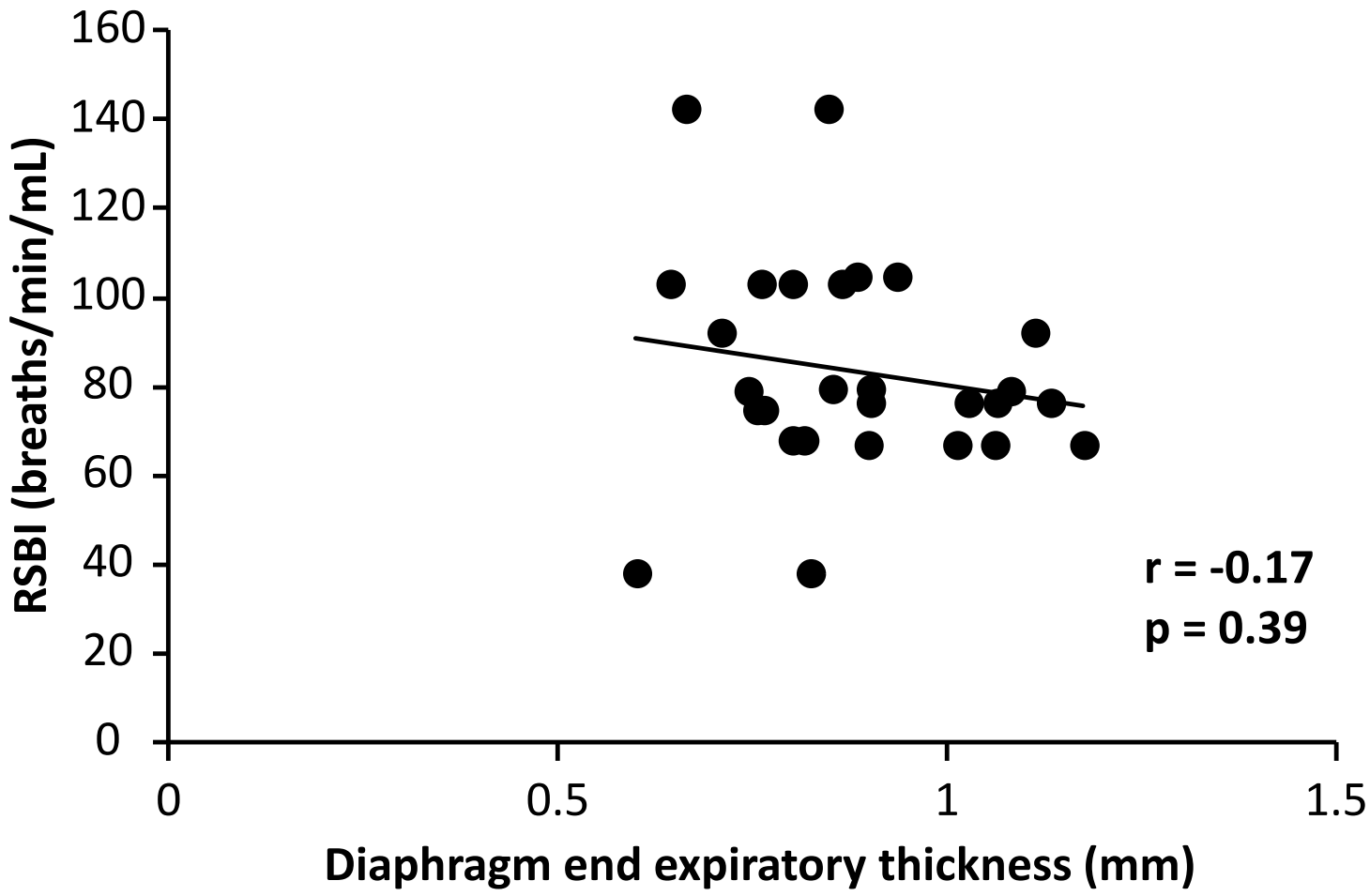
160
140
120
100
80
60
40
20
0
RSBI (breaths/min/mL)
0
0.5
1
1.5
Diaphragm end expiratory thickness (mm)
r = -0.17
p = 0.39

Parameters	Mean ± SD (min-max)	CV (%)
Weight (g)	386 ± 79 (291-599)	20
T_I (ms)	199 ± 39 (131-298)	20
T_E (ms)	396 ± 133 (256-785)	34
V_M (mL/min)/100g	44.01 ± 10.52 (26.87-72.67)	8.95
V_T (mL)/100g	0.39 ± 0.03 (0.32-0.48)	23.90
Respiratory Rate (breaths/min)	113 ± 23 (72-166)	21
RSBI (Respiratory Rate/ V_T)	293 ± 70 (187-425)	24

Table 1. Whole body plethysmography in unanesthetized eupneic rats. Inspiratory time (T_I), expiratory time (T_E), minute ventilation (V_M), tidal volume (V_T), RSBI (Rapid Shallow Breathing index), minimum (min) and maximum (max). CV = coefficient of variation. Sample size (n) =14.

combinations	CC (right rectus abdominis area)	CC (right rectus abdominis thickness)	CC (right diaphragm inspiratory thickness)	CC (right diaphragm inspiratory motion)
Variability (inter-operator)	0.93 (p = 0.022)	0.885 (p = 0.046)	0.873 (p = 0.050)	0.962 (p = 0.009)
Reproducibility (intra-operator n°1)	0.916 (p = 0.043)	0.971 (p = 0.014)	0.912 (p = 0.049)	0.971 (p = 0.015)

Table 2. Correlation Coefficient (CC) for reproducibility intra-operator and variability inter-operator. Sample size (n) = 4.

Analysis	Ultrasound (mm^2)	Histology (mm^2)	Bias	SD of bias	95% LOA	Estimated sample size
Right rectus abdominis area	23.00 ± 1.02 (22.14-24.04)	21.90 ± 1.95 (19.13-23.73)	1.10	2.82	-4.42 to 6.62	4
Left rectus abdominis area	22.80 ± 1.00 (21.54-23.73)	21.78 ± 0.65 (20.85-22.38)	1.02	0.92	-0.79 to 2.82	4

Table 3. Agreement and correlation between ultrasound and histology measurements. Limits of agreement (LOA).